ELSEVIER

Biophysical Chemistry 54 (1995) 237–251

Biophysical Chemistry

Pre-steady-state kinetics and modelling of the oxygenase and cyclooxygenase reactions of prostaglandin endoperoxide synthase

Marica Bakovic, H. Brian Dunford *

Department of Chemistry, University of Alberta, Edmonton, Alberta, Canada, T6G 2G2

Received 27 June 1994; revised 26 August 1994; accepted 17 October 1994

Abstract

The pre-steady-state kinetics of the prostaglandin endoperoxide synthase oxygenase reaction with eicosadienoic acids and the cyclooxygenase reaction with arachidonic acid were investigated by stopped-flow spectrophotometry at 426 nm, an isosbestic point between native enzyme and compound I. A similar reaction mechanism for both types of catalysis is defined from combined kinetic experiments and numerical simulations. In the first step a fatty acid hydroperoxide reacts with the native enzyme to form compound I and the fatty acid hydroxide. In the second step the fatty acid reduces compound I to compound II and a fatty acid carbon radical is formed. This is followed by two fast steps: (1) the addition of either one molecule of oxygen (the oxygenase reaction) or two molecules of oxygen (the cyclooxygenase reaction) to the fatty acid carbon radical to form the corresponding hydroperoxyl radical, and (2) the reaction of the hydroperoxyl radical with compound II to form the fatty acid hydroperoxide and a compound I–protein radical. A unimolecular reaction of the compound I–protein radical to reform the native enzyme is assumed for the last step in the cycle. This is a slow reaction not significantly affecting steps 1 and 2 under pre-steady-state conditions. A linear dependence of the observed pseudo-first-order rate constant, k_{obs}, on fatty acid concentration is quantitatively reproduced by the model for both the oxygenase and cyclooxygenase reactions. The simulated second order rate constants for the conversion of native enzyme to compound I with arachidonic or eicosadienoic acids hydroperoxides as a substrate are 8×10^7 and 4×10^7 M^{-1} s^{-1}, respectively. The simulated and experimentally obtained second-order rate constants for the conversion of compound I to compound II with arachidonic and eicosadienoic acids as a substrate are 1.2×10^5 and 3.0×10^5 M^{-1} s^{-1}, respectively.

Keywords: Prostaglandin endoperoxide synthase; Arachidonic acid; Eicosadienoic acid; Pre-steady-state kinetics; Computer simulation

1. Introduction

One of the most intriguing aspects of prostaglandin biosyntheses is the ability of prostaglandin endoperoxide synthase (PGH synthase) to catalyze both the oxygenation of arachidonic acid (20:4) to prostaglandin G_2 (PGG_2) and the reduction of PGG_2 to prostaglandin H_2 (PGH_2). These two reactions have been described as cyclooxygenase and peroxidase reactions; and there is a great deal of discussion today as to whether they occur semi-independently or sequentially in the overall process of PGH_2 synthesis.

It is now evident that the peroxidase reaction is a single elementary reaction in which an oxygen atom

* Corresponding author.

SSDI 0301-4622(94)00135-9

is transferred from the –OOH group of PGG_2 to native PGH synthase resulting in an iron(IV) porphyrin π-cation radical (compound I) and PGH_2 formation [1], a reaction typical of all heme containing peroxidases [2]. The implication is that the so-called cyclooxygenase reaction occurs first (Eq. 1) and is followed by the peroxidase reaction (Eq. 2):

$$20{:}4 + 2O_2 \xrightarrow{\text{cyclooxygenase}} PGG_2 \quad (1)$$

$$\text{PGH synthase} + PGG_2 \xrightarrow{\text{peroxidase}} \text{compound I} + PGH_2 \quad (2)$$

On the other hand it is well known that for the initiation of oxygen consumption in the overall reaction, traces of a hydroperoxide are needed, and furthermore that classical peroxidase reducing substrates can cause dramatic changes in the rates of oxygen consumption, implying that the peroxidase function of the enzyme plays a key role in the cyclooxygenase reaction.

A tyrosyl–radical mechanism has been proposed for the cyclooxygenase reaction [3,4]. Compound I formed in Eq. 2 converts spontaneously by an intramolecular one-electron transfer to an iron(IV) tyrosyl radical (Eq. 3):

$$\text{compound I} \rightarrow \text{compound I–Tyr}^{\cdot} \quad (3)$$

According to this hypothesis the tyrosyl radical then initiates the cyclooxygenase reaction as depicted in Eqs. 4–6:

$$\text{compound I–Tyr}^{\cdot} + 20{:}4 \rightarrow \text{compound II} + 20{:}4^{\cdot} \quad (4)$$

$$20{:}4^{\cdot} + 2O_2 \rightarrow PGG_2^{\cdot} \quad (5)$$

$$\text{compound II} + PGG_2^{\cdot} \rightarrow \text{compound I–Tyr}^{\cdot} + PGG_2 \quad (6)$$

Initially, the tyrosyl radical abstracts the hydrogen atom from 20:4 producing the carbon radical $20{:}4^{\cdot}$ and compound II (Eq. 4). The carbon radical is then trapped by two molecules of oxygen producing the $PGG_2^{\cdot}$ radical (Eq. 5); and finally, PGG_2 is formed by hydrogen atom donation from a tyrosyl residue of compound II and the compound I–tyrosyl radical is regenerated (Eq. 6). The main implication of the tyrosyl radical mechanism is that once initiated, the branched-chain free radical reaction (Eqs. 4–6) can continue independently of the normal proxidase cycle.

Recently we obtained results showing that there is a fixed and constant (2:1) ratio between the rates of reaction of a conventional peroxidase reducing substrate ferulic acid (RH) and the cyclooxygenase substrate 20:4 [5] that are incompatible with the branched-chain tyrosyl radical hypothesis. The corresponding mechanism is shown in Eqs. 2, 3a and 5–8:

$$\text{PGH synthase} + PGG_2 \rightarrow \text{compound I} + PGH_2 \quad (2)$$

$$\text{compound I} + 20{:}4 \rightarrow \text{compound II} + 20{:}4^{\cdot} \quad (3a)$$

$$20{:}4^{\cdot} + 2O_2 \rightarrow PGG_2^{\cdot} \quad (5)$$

$$\text{compound II} + PGG_2^{\cdot} \rightarrow \text{compound I–Tyr}^{\cdot} + PGG_2 \quad (6)$$

$$\text{compound I–Tyr}^{\cdot} + RH \rightarrow \text{compound II} + R^{\cdot} \quad (7)$$

$$\text{compound II} + RH \rightarrow \text{PGH synthase} + R^{\cdot} \quad (8)$$

Compound I is not converted spontaneously to the compound I–tyrosyl radical (Eq. 3). Compound I rather abstracts a hydrogen atom from 20:4 (Eq. 3a) and forms compound II and the carbon radical $20{:}4^{\cdot}$. The following two steps are the same as in the branched-chain tyrosyl radical mechanism (Eqs. 5 and 6). The classical electron (hydrogen atom) donor RH (Eqs. 7 and 8) reacts with both the compound I–tyrosyl radical and compound II and the native enzyme is regenerated. This mechanism implies an intimate relation between peroxidase and cyclooxygenase activities of PGH synthase and shows how electron donors other than fatty acid can facilitate the cycle and help prevent inactivation.

The hypothetical role for the compound I–tyrosyl radical to initiate the oxygenation of fatty acids can be tested kinetically under pre-steady-state conditions by following the rate of its formation at 426 nm, an isosbestic point between native enzyme and compound I, as a function of fatty acid concentration. The spontaneous formation of the compound I–tyrosyl radical from compound I (Eq. 3) is a unimolecular elementary reaction and the rate of its formation should be independent on the fatty acid concentration. Here we report that in the absence of classical peroxidase electron donors (the spontaneous cyclooxygenase reaction) the reaction in Eq. 3 does

not occur. Rather, the disappearance of compound I is a function of fatty acid concentration as shown in Eq. 3a. The latter reaction was proposed previously for the combined cyclooxygenase–peroxidase reaction [5]. The compound I–tyrosyl radical (or electronically equivalent protein radical) is formed later in a bimolecular reaction between the hydroperoxyl radical and compound II (Eq. 6).

2. Materials and methods

2.1. Materials

All reagents used in this study were of the highest grade available. Arachidonic (20:4), eicosadienoic (20:2) and docosahexaenoic (22:6) acids, indomethacin and hematin were purchased from Sigma; phenol from British Drug House; DE 53 ion-exchange chromatography gel from Whatman; Tween 20 from J.T. Baker. 20:4, 20:2 and 22:6 were dissolved in deaerated absolute ethanol and kept in small portions under nitrogen at $-70°$ C. The aliquots of 20:2 stock solutions were dried with nitrogen and oxidized with oxygen for different periods of time (0–3 hours). After specific times, the excess of oxygen was removed with nitrogen and the oxidized samples of 20:2 were redissolved in deaerated absolute ethanol and kept at $-70°$ C before use. The concentration of the conjugated diene hydroperoxide formed by the oxidation of 20:2 (HOO–20:2) was measured spectrophotometrically at 235 nm using an ϵ of 2.4×10^4 M^{-1} cm^{-1} [6,7].

PGH synthase was isolated from ram seminal vesicle microsomes using the procedure as published [8,9]. Measurements of protein content were conducted by the BioRad protein assay using bovine serum albumin as a standard. Enzyme concentrations were determined spectrophotometrically using an ϵ of 123 mM^{-1} cm^{-1} [10].

2.2. Oxygen electrode measurements

Cyclooxygenase activity was determined by measuring oxygen consumption in the reaction of 20:4 with PGH synthase at 30° C in 0.1 M phosphate buffer, pH 8.0, using a Yellow Spring Instruments Model 53 oxygen monitor equipped with a Clark-type polarographic electrode. The oxygen concentration dissolved in the buffer was 230 μM at 30° C [11]. The specific activity of the enzyme was calculated by assuming that 2 mol of oxygen were consumed per mole of 20:4. The enzyme preparations from two isolations were roughly a 30/70 mixture of holo- and apo-enzyme having a specific cyclooxygenase activity of 37 and 44 μM 20:4 mg protein^{-1} min^{-1} in the presence of 1 μM hematin and 1 mM phenol. The holo/apo enzyme preparations were reconstituted with hematin (2.5 – fold more hematin was added to what was initially present in the holo/apo enzyme) immediately after isolation. The reconstituted enzyme was stored at $-70°$ C without changing the heme content or enzyme activity during the experiments.

2.3. Rapid-scan and stopped-flow experiments

The experiments were performed on a Photal RA 601 Rapid Reaction Analyzer equipped with 1-cm cells thermostated at $30 \pm 0.5°$ C. The absorption spectra were measured by means of a multichannel photodiode array photometer, memorized in a computer system with the corresponding replica plotted on an Epson VP-550 recorder. Soret band absorption of the heme of PGH synthase was utilized for rapid scanning of the transformation of the enzyme species during the reactions.

Stopped-flow kinetic analysis was performed at a single wavelength from the Soret region, i.e., at 426 nm, an isosbestic point between the native enzyme and compound I [1,4,12,13].

For the assays with 20:4, fixed amounts of PGH synthase (0.25 μM) and oxygen (230 μM) were reacted with different amounts of 20:4 (5.5–60 μM). The anaerobically stored stock solution of 20:4 contained trace amounts of hydroperoxide capable of activation of the cyclooxygenase reaction. Any change in [20:4] in the assay mixture automatically caused changes in the hydroperoxide concentration.

To overcome the difficulty of not being able to control hydroperoxide concentration, we performed a different type of experiment with 20:2. A series of stock solutions containing various amounts of 20:2 and hydroperoxide HOO–20:2 were prepared by oxidizing 20:2 samples with oxygen. Thus, it was possible to keep the [HOO–20:2] constant while the [20:2]

was varied. Single assays under pseudo-first-order conditions were carried out at constant concentration of enzyme (0.25 μM), oxygen (230 μM) and hydroperoxide (2.5 μM), and varied concentrations of 20:2 (5.3–99 μM).

The rest of the procedure was identical for both 20:4 and 20:2. One cell of the Rapid Reaction Analyzer contained PGH synthase dissolved in 0.1 M phosphate buffer, pH 8.0. The enzyme solution was incubated 3 min at 30° C before reaction. The other cell contained the fatty acid/hydroperoxide mixture dissolved in the same buffer. The buffer solution was also preincubated for 3 min at 30° C and fatty acid/hydroperoxide were added to the cell immediately before measurements. Mixing of solutions to cause the reaction was complete in 2 ms. Duplicate or triplicate sets of experiments were performed for identical reaction mixtures and usually 5–8 reproducible kinetic traces were collected for each set. The relative standard deviation was in the range of 7–10%.

2.4. Data analysis

The observed pseudo-first-order rate constants, k_{obs}, obtained from the exponential curve fits to the kinetic traces at 426 nm was plotted as a function of [fatty acid]. Different mechanistic models were simulated on a Macintosh Plus 40SC computer. A system of first-order differential equations was defined and numerically integrated by the fourth-order Runge–Kutta method using the GRAF PLOT general plotting program kindly provided by Dr. R.B. Jordan, University of Alberta. Numerical integration using the GRAF PLOT program was conducted by an iterative process, varying one rate constant at a time. The ranges of the rate constants were assigned based on the experimental values obtained in this study and on those already published [3,4,12]. The k_{obs} values were determined from the computed kinetic parameters and compared with those obtained experimentally.

2.5. Experiments with indomethacin and 22:6

The effect of the cyclooxygenase inhibitors indomethacin and 22:6 on the values of the observed pseudo-first-order rate constant, k_{obs}, was monitored at constant concentrations of enzyme (0.25 μM), oxygen (230 μM) and 20:4 (50 μM), and various concentrations of indomethacin or 22:6. In one cell of the stopped-flow apparatus the enzyme and inhibitor were incubated 2 min in 0.1 M phosphate buffer, pH 8.0, at 30°. In the other, 20:4 was added immediately before measurements. Reproducible kinetic traces were obtained within the next 2 min. If the times for the measurements were prolonged and/or not controlled the traces were not very reproducible because of time-dependent inhibitory processes, an irreversible inhibition with indomethacin and possibly the autooxidation of 22:6 [14–17].

3. Results

3.1. Spectral changes during the cyclooxygenase and oxygenase reactions

In preliminary experiments with 20:4 as a substrate (the cyclooxygenase reaction) we obtained identical changes in the enzyme Soret spectra as were obtained previously [1,4,12,13]. Typically, intermediate II (compound II or compound I–Tyr·) was formed in a mixture with native enzyme. The native enzyme has an absorption maximum at 410 nm. Initially there is an absorbance decrease and an isosbestic point at 420 nm appears indicating the presence of a steady-state mixture of intermediate II and native enzyme. The spectrum usually becomes complicated with heme bleaching at higher fatty acid concentrations and/or at longer times. Fig. 1 shows, for the first time, changes in the PGH synthase Soret spectra obtained for the oxygenase reaction with 20:2. The spectral changes are qualitatively the same as in the cyclooxygenase reaction with 20:4. As the existence of the isosbestic point at 420 nm indicates, a mixture of native enzyme and intermediate II was present. For spectral measurements only, oxygen was partially removed from the buffer before a 1:1 ratio of the enzyme and HOO–20:2 (0.25 μM/0.25 μM) and an excess of 20:2 (37 μM) were introduced to initiate the reaction. Under these conditions the oxygen is a limiting reagent and the reaction was slowed down to the level at which it was possible to apply the conventional spectroscopy to obtain the changes in the enzyme spectra; no bleaching of the heme

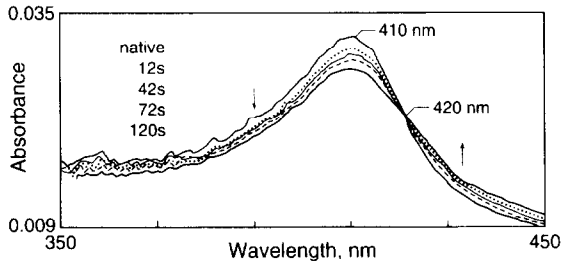

Fig. 1. PGH synthase optical spectra recorded during the oxygenase reaction. The reaction was carried out in 0.1 M phosphate buffer, pH 8.0, at 22° C. Before the enzyme (0.25 μM), 20:2 (37 μM) and HOO–20:2 (0.25 μM) were mixed O_2 was partially removed from the buffer by N_2. The spectra have an isosbestic point at 420 nm indicating the presence of a mixture of the native enzyme and intermediate II (compound I–Tyr˙ or compound II). The arrows show the direction of absorbance change with time.

occurred during 2 min. This experiment shows that the PGH synthase spectral intermediates can be obtained not only at low temperatures with fast techniques [1,4,12,13] but also at room temperature with conventional methods if lower amounts of oxygen and hydroperoxide are used. For kinetic measurements, the solutions were saturated with oxygen.

Rapid-scan method was used in a routine control of the experimental conditions before the stopped-flow kinetic measurements were performed. In these experiments the oxygen concentration (230 μM dissolved in the buffer at 30° C) was not changed and the hydroperoxide was in the excess of the enzyme. Except that the reactions were faster, they resulted in no principal difference from the spectra shown in Fig. 1.

3.2. Effects of 20:4 and 20:2 on the intermediate II formation

The isosbestic point between the native enzyme and compound I at 426 nm has been clearly identified under transient-state conditions for the peroxidase reactions of native enzyme with hydroperoxides [1,4]. The 426 nm wavelength has been used for monitoring the conversion of compound I to intermediate II, compound I–Tyr˙ [4] in a reaction initiated by PGG_2 and with no fatty acid present. We followed the same reaction as a function of [fatty acid]. A dependence of the rate of the formation of intermediate II from [fatty acid] was obtained with both 20:4 and 20:2 as substrates. Fig. 2 shows kinetic traces obtained with 20:4. At the lowest [20:4] the kinetic trace shows a pre-steady-state phase in which there is an induction period (lag phase) before the intermediate II started to form (Fig. 2A). At longer times the steady-state is established. The presence of the lag phase indicates that yet another intermediate (compound I) was formed before intermediate II. If the [fatty acid] is higher the lag phase is diminished but does not disappear from the kinetic traces (Fig. 2B and C). The dependence of the rate of formation of intermediate II on [fatty acid] would not be expected for the unimolecular formation of compound I–Tyr˙, which would have a spectrum identical to

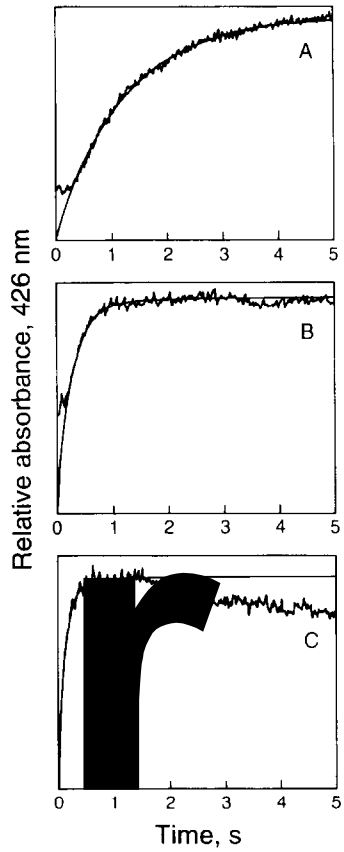

Fig. 2. Effect of 20:4 on the rates of the intermediate II formation. Absorbance changes were followed at 426 nm, an isosbestic point between native enzyme and compound I. (A) 5.5, (B) 30, (C) 60 μM of 20:4 reacted with 0.25 μM PGH synthase in 0.1 M phosphate buffer, pH 8.0, at 30° C. The observed pseudo-first-order rate constant, k_{obs}, is: (A) 0.813, (B) 3.50, and (C) 7.36 s^{-1}.

that of compound II (Eq. 3) [4]. Both the induction phase and the pre-steady-state phase were faster for 30 and 60 μM 20:4 than at 5.5 μM 20:4, indicating that intermediate II formation is not unimolecular but is dependent upon fatty acid concentration.

The stopped-flow and rapid-scan studies of the reaction of PGH synthase with different [20:4] were extended to longer times (50 s) after the steady-state conditions had been established (data not shown). These experiments show that the return of intermediate II to the native state (partly also shown in Fig. 2C as a drop in absorbance after the steady state has been reached) is complicated by enzyme bleaching. Thus, the inactivation events occur after, not before, intermediate II is formed. We were not interesting in the inactivation process; we followed the events before the steady-state conditions were established.

3.3. Inhibition of the intermediate II formation

The cyclooxygenase inhibitors indomethacin and 22:6 inhibited the rate of the intermediate II formation as indicated in Fig. 3. The concentration of indomethacin necessary to cause a 50% decrease of the observed pseudo-first-order rate constant, k_{obs}, is 2.3 μM when the reaction was performed with 50 μM 20:4 and 0.25 μM enzyme. The fatty acid 22:6 is a significantly weaker inhibitor of intermediate II formation than indomethacin. No linear decrease in k_{obs} as a function of [22:6] was obtained; k_{obs} levelled off at 20–60 μM of [22:6] at a value approximately 44% lower than in the absence of 22:6.

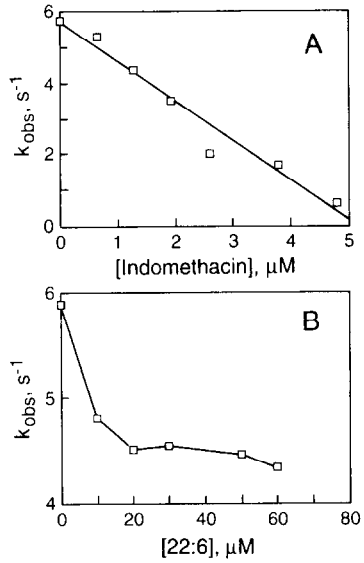

Fig. 3. Effects of cyclooxygenase inhibitors on the observed pseudo-first-order rate constant, k_{obs}, for the reaction of 50 μM 20:4 and 0.25 μM enzyme. Other conditions are the same as in Fig. 2. (A) 0–4.8 μM indomethacin and (B) 0–60 μM 22:6.

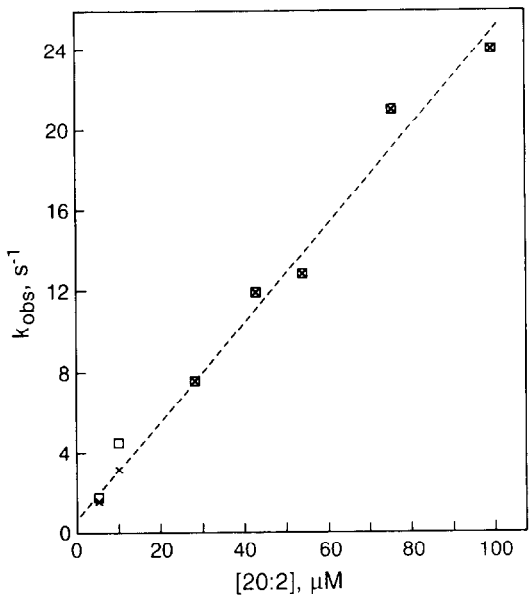

Fig. 4. Comparison of the experimental (□) and simulated (+) k_{obs} versus [20:2]. Theoretical k_{obs} were calculated according to the model in Scheme 1 by using the following kinetic parameters: $k_1 = 4\times10^7$; $k_2 = 3\times10^5$ M^{-1} s^{-1}; and $k_3 = 3\times10^{-3}$ s^{-1}. Initial conditions: $[E]_0 = 0.25$ μM, $[AH]_0 = 5.3$–90 μM, $[AOOH]_0 = 2.5$ μM.

3.4. Kinetic model for the oxygenase reaction

The observed pseudo-first-order rate constant, k_{obs}, obtained from the pre-steady-state kinetic measurements was a linear function of [20:2], a characteristic typical of bimolecular reactions (Fig. 4). The experiments were performed at constant [PGH synthase] and 10-fold higher [HOO–20:2]. Only [20:2] was varied in the reaction mixtures. The experimental conditions were essentially pseudo-first-order and single exponential curves were obtained at 426 nm. Analysis of the [20:2] dependence of the pre-steady-state kinetics led to the following proposal of a

mechanism of the oxygenase pathway of PGH synthase.

Scheme 1:

$$E + AOOH \xrightarrow{k_1} E\text{-}I + AOH \quad (9)$$

$$E\text{-}I + AH \xrightarrow{k_2} E\text{-}II + A^{\cdot} \quad (10)$$

$$A^{\cdot} + O_2 \xrightarrow{k_{O_2}} AOO^{\cdot} \quad (11)$$

$$E\text{-}II + AOO^{\cdot} \xrightarrow{k_{AOO^{\cdot}}} E\text{-}I\text{-}X^{\cdot} + AOOH \quad (12)$$

$$E\text{-}I\text{-}X^{\cdot} \xrightarrow{k_3} E \quad (13)$$

The above model predicts the existence of three enzyme intermediates during the oxygenase reaction, compound I (E-I), compound II (E-II) and compound I–protein radical (E-I–X$^{\cdot}$). All steps are bimolecular except the last one: native enzyme (E) reacts with fatty acid hydroperoxide AOOH, compound I (E-I) with fatty acid AH, and compound II (E-II) with fatty acid hydroperoxyl radical AOO$^{\cdot}$. A unimolecular last step was assumed for the spontaneous decay of the protein radical E-I–X$^{\cdot}$ to the native enzyme. This step is a secondary reaction which occurs at much lower rates then the formation of the intermediates.

A set of seven differential equations corresponding to the mechanism in Scheme 1 is defined as follows:

$$d[E]/dt = k_3[E\text{-}I\text{-}X^{\cdot}] - k_1[E][AOOH] \quad (14)$$

$$d[E\text{-}I]/dt = k_1[E][AOOH] - k_2[E\text{-}I][AH] \quad (15)$$

$$d[E\text{-}II]/dt = k_2[E\text{-}I][AH] - k_{AOO^{\cdot}}[E\text{-}II][AOO^{\cdot}] \quad (16)$$

$$d[E\text{-}I\text{-}X^{\cdot}]/dt = k_{AOO^{\cdot}}[E\text{-}II][AOO^{\cdot}] - k_3[E\text{-}I\text{-}X^{\cdot}] \quad (17)$$

$$d[A^{\cdot}]/dt = k_2[E\text{-}I][AH] - k_{O_2}[A^{\cdot}][O_2] \quad (18)$$

$$d[AOO^{\cdot}]/dt = +k_{O_2}[A^{\cdot}][O_2] - k_{AOO^{\cdot}}[E\text{-}II][AOO^{\cdot}] \quad (19)$$

$$d[AOOH]/dt = k_{AOO^{\cdot}}[E\text{-}II][AOO^{\cdot}] - k_1[E][AOOH] \quad (20)$$

By setting differential Eqs. 18 and 19 to zero, one can find the values of the steady-state concentrations of the fatty acid carbon radical A$^{\cdot}$ and the fatty acid hydroperoxyl radical AOO$^{\cdot}$:

$$[A^{\cdot}] = \frac{k_2[E\text{-}I][AH]}{k_{O_2}[O_2]} \quad (21)$$

$$[AOO^{\cdot}] = \frac{k_2[E\text{-}I][AH]}{k_{AOO^{\cdot}}[E\text{-}II]} \quad (22)$$

Substituting [A$^{\cdot}$] and [AOO$^{\cdot}$] in Eqs. 16, 17 and 20 the model is reduced to four differential equations as follows:

$$d[E]/dt = k_3[E\text{-}I\text{-}X^{\cdot}] - k_1[E][AOOH] \quad (23)$$

$$d[E\text{-}I]/dt = k_1[E][AOOH] - k_2[E\text{-}I][AH] \quad (24)$$

$$d[E\text{-}I\text{-}X^{\cdot}]/dt = k_2[E\text{-}I][AH] - k_3[E\text{-}I\text{-}X^{\cdot}] \quad (25)$$

$$d[AOOH]/dt = k_2[E\text{-}I][AH] - k_1[E][AOOH] \quad (26)$$

Assuming that A$^{\cdot}$ and AOO$^{\cdot}$ are under steady-state conditions the d[E-II]/dt (Eq. 16) becomes zero automatically.

Fig. 5 shows some possible solutions for the oxygenase reaction calculated by the model in Scheme 1 by using different combinations of the rate

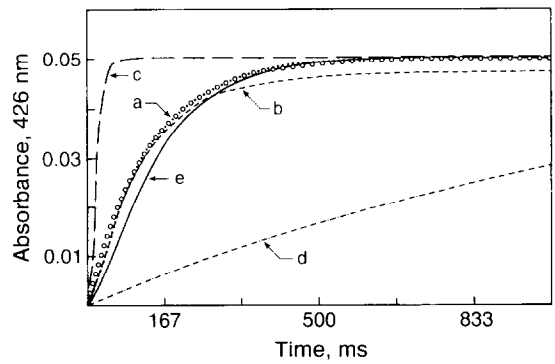

Fig. 5. Sensitivity of the kinetic model proposed for the oxygenase reaction on the kinetic rate constants k_1, k_2 and k_3 according to the pathway in Scheme 1. (○) The experimentally obtained exponential curve with $k_{obs} = 7.62\ s^{-1}$; (a) $k_1 = 4\times10^7\ M^{-1}\ s^{-1}$, $k_2 = 3\times10^5\ M^{-1}\ s^{-1}$, $k_3 = 5\times10^{-3}\ s^{-1}$; (b) $k_1 = 4\times10^7\ M^{-1}\ s^{-1}$, $k_2 = 3\times10^5\ M^{-1}\ s^{-1}$, $k_3 = 0.5\ s^{-1}$; (c) $k_1 = 4\times10^7\ M^{-1}\ s^{-1}$, $k_2 = 3\times10^6\ M^{-1}\ s^{-1}$, $k_3 = 5\times10^{-3}\ s^{-1}$; (d) $k_1 = 4\times10^7\ M^{-1}\ s^{-1}$, $k_2 = 3\times10^4\ M^{-1}\ s^{-1}$, $k_3 = 5\times10^{-3}\ s^{-1}$; (e) $k_1 = 1\times10^6\ M^{-1}\ s^{-1}$, $k_2 = 3\times10^5\ M^{-1}\ s^{-1}$, $k_3 = 5\times10^{-3}\ s^{-1}$; $[E]_0 = 0.25\ \mu M$, $[AH]_0 = 28.3\ \mu M$, and $[AOOH]_0 = 2.5\ \mu M$

constants k_1, k_2 and k_3. The rate constants were changed one at a time. The calculated kinetic trace is most sensitive to the value of k_2 (Fig. 5, c and d), moderately sensitive to k_1 (Fig. 5, e) and least sensitive to k_3 (Fig. 5, a and b). The rate constant k_2 seriously affects the shape of the whole trace; k_1 mostly affects the exponential part of the trace (the pre-steady-state phase after the initial lag) while k_3 predominantly influences the amplitude of the trace (the steady-state phase).

The observed exponential increase in absorbance at 426 nm (Fig. 6A) was fully reproduced by the model as the increase in the concentration of E-I–X$^{\cdot}$ species (Fig. 6B). Changes in concentrations against time for other two main species E, E-I are also shown in Fig. 6B. The best fit for this and other experiments with 20:2 were obtained with $k_1 = 4 \times 10^7$ M^{-1} s^{-1}, $k_2 = 3 \times 10^5$ M^{-1} s^{-1} and $k_3 = 3$ x10^{-3} s^{-1}. The computer simulated and experimentally obtained k_{obs} are plotted as a function of [20:2] in Fig. 4.

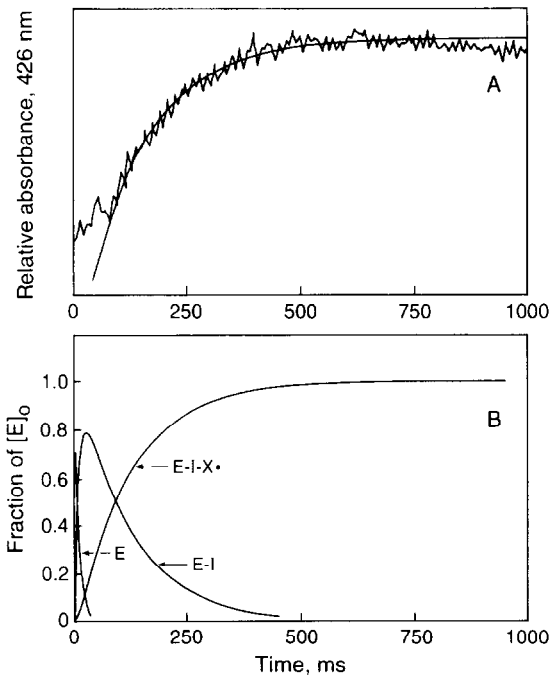

Fig. 6. Absorbance changes and curve fit of the kinetic trace at 426 nm (A) and simulated time courses (B) of the enzyme species during the reaction of PGH synthase and 20:2. (A) The reaction mixture contained 28.3 μM 20:2, 2.5 μM HOO–20:2 and 0.25 μM enzyme ([E]$_0$ in B). (B) The time profiles for native enzyme (E), compound I (E-I) and compound I–protein radical (E-I–X$^{\cdot}$) calculated by numerical integration according to the model shown in Scheme 1 with the following rate constants $k_1 = 4 \times 10^7$ and $k_2 = 3 \times 10^5$ M^{-1} s^{-1}; $k_3 = 3$x10^{-3} s^{-1} and $k_{obs} = 7.62$ s^{-1}.

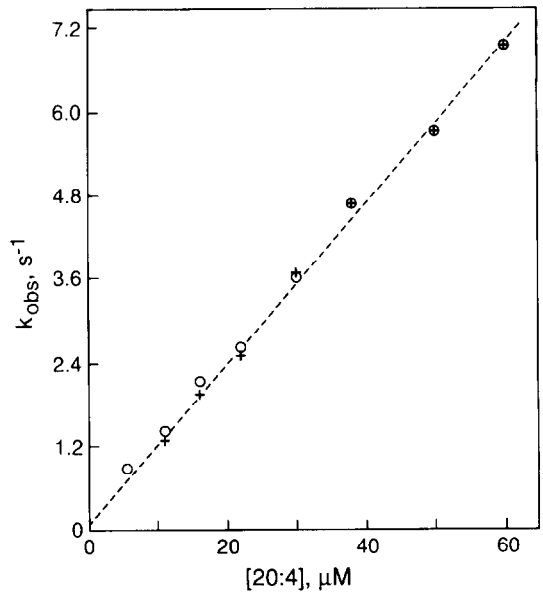

Fig. 7. Experimental (○) and simulated (+) data showing the linear dependence of k_{obs} from [20:4]. Theoretical k_{obs} were calculated according to the kinetic model in Scheme 2 by using the following rate constants $k_1 = 8 \times 10^7$ M^{-1} s^{-1}, $k_2 = 1.2 \times 10^5$ M^{-1} s^{-1}, and $k_3 = 3$ x10^{-3} s^{-1} and initial conditions: [E]$_0$ = 0.25 μM, [AH]$_0$ = 5.5–60 μM.

3.5. Kinetic models for the cyclooxygenase reaction

The experimental plot shown in Fig. 7 demonstrates that there is a similar linear relationship between k_{obs} and [20:4] for the cyclooxygenase reaction as for the oxygenase reaction (Fig. 4). However, the principal difference between the two studies was that in the cyclooxygenase reaction the initial concentration of hydroperoxide was not constant. Due to the presence of an unknown amount of a contaminant hydroperoxide in stock solutions of 20:4, whenever the initial [20:4] was changed the initial [hydroperoxide] also changed.

An experimentally obtained kinetic trace for the cyclooxygenase reaction and the best simulated trace for the same reaction are shown in Fig. 8. The simulated trace was obtained according to the mech-

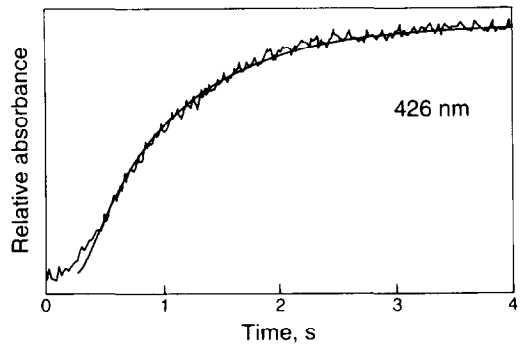

Fig. 8. Absorbance change at 426 nm and simulated time course for compound I–protein radical (E-I–X$^{\cdot}$) formation during the reaction of PGH synthase and 20:4. The reaction mixture contained 11 μM 20:4 and 0.25 μM enzyme. The time profile for E-I–X$^{\cdot}$ (smooth curve) was calculated by numerical integration according to the model in Scheme 2 with the following rate constants $k_1 = 8\times10^7$ and $k_2 = 1.2\times10^5$ M^{-1} s^{-1}; $k_3 = 3\times10^{-3}$ s^{-1}; the experimentally measured $k_{obs} = 1.27$ s^{-1} and initial conditions: $[AH]_0 = 11$ μM, $[A(O_2)OOH]_0 = 0.39$ μM, and $[E]_0 = 0.25$ μM. Thus an excellent fit is obtained to the dominant burst phase. Zero time for the simulation curve is the time at which E-I–X$^{\cdot}$ starts to form. Therfore the time scale for the simulation curve is shifted by 0.25 s because of the poor fit to the initial lag phase, in which E-I–X$^{\cdot}$ is not being formed.

anism which predicts that compound I reacts with 20:4 and thus initiates the cyclooxygenase reaction as follows:

Scheme 2:

$$E + A(O_2)OOH \xrightarrow{k_1} E\text{-}I + A(O_2)OH \quad (27)$$

$$E\text{-}I + AH \xrightarrow{k_2} E\text{-}II + A^{\cdot} \quad (28)$$

$$A^{\cdot} + 2O_2 \xrightarrow{k_{O_2}} A(O_2)OO^{\cdot} \quad (29)$$

$$E\text{-}II + A(O_2)OO^{\cdot} \xrightarrow{k_{AOO}} E\text{-}I\text{-}X^{\cdot} + A(O_2)OOH \quad (30)$$

$$E\text{-}I\text{-}X^{\cdot} \xrightarrow{k_3} E \quad (31)$$

In Scheme 2, $A(O_2)OOH$ and $A(O_2)OH$ are prostaglandin G_2 (hydroperoxide–endoperoxide) and prostaglandin H_2 (hydroxy–endoperoxide), and AH is 20:4. The mechanism for the cyclooxygenase reaction is identical to that for the oxygenase reaction (Scheme 1) except that two molecules of oxygen are necessary to produce the hydroperoxide endoperoxide radical $A(O_2)OO^{\cdot}$. The mechanism in Scheme 2 is defined by a similar set of differential equations as in Scheme 1. After applying the steady-state approximation for $[A^{\cdot}]$, $[A(O_2)OO^{\cdot}]$ and [E-II] the cyclooxygenase system is governed by an identical set of working equations (Eqs. 23–26) as the oxygenase system.

For the best simulation shown in Fig. 8 we assigned the values for the rate constant k_1 of 8×10^7 M^{-1} s^{-1}, based on the reported value for a similar 20:4-hydroperoxide, 15-hydroperoxy eicosatetraenoic acid (15-HPETE) of 7.1×10^7 M^{-1} s^{-1} at 25° C [14], for k_2 1.2×10^5 M^{-1} s^{-1} and $k_3 = 3\times10^{-3}$ s^{-1}. We estimated the initial hydroperoxide concentration while keeping other parameters constant. It appeared that the best estimate for the hydroperoxide concentration was 3.4–3.5% of the initial [20:4]. This approximates the amount of hydroperoxide initially present in the 20:4 stock solutions. According to the manufacturer the purity of 20:4 was 99% but we knew from the spectroscopic measurements with similarly sensitive 20:2 (99% purity) that some autooxidation occurs during the storage and the preparation of the stock solutions leading to the initial presence of 2–3% of HOO–20:2 in 20:2 stock solutions. The theoretical and experimental plots of k_{obs} against [20:4] obtained for a series of [20:4] were identical when the above conditions were applied (Fig. 7).

The second mechanism tested, shown below in Scheme 3, is based on the tyrosyl–radical hypothesis in which compound I–tyrosyl radical reacts with 20:4 and thus initiates the cyclooxygenase cycle. Instead of specifying the nature of the intermediate as the compound I–tyrosyl radical we would rather call it the compound I–protein radical (E-I–X$^{\cdot}$); no electronic nor spectroscopic differences in the heme part of the two possible intermediates exists and it does not make any principal change in the mechanism.

Scheme 3:

$$E + A(O_2)OOH \xrightarrow{k_1} E\text{-}I + A(O_2)OH \quad (32)$$

$$E\text{-}I \xrightarrow{k_{2a}} E\text{-}I\text{-}X^{\cdot} \quad (33)$$

$$E\text{-}I\text{-}X^{\cdot} + AH \xrightarrow{k_2} E\text{-}II + A^{\cdot} \quad (34)$$

$$A^{\cdot} + 2O_2 \xrightarrow{k_{O_2}} A(O_2)OO^{\cdot} \quad (35)$$

$$E\text{-II} + A(O_2)OO^{\cdot} \xrightarrow{k_{AOO}} E\text{-I–X}^{\cdot} + A(O_2)OOH \quad (36)$$

$$E\text{-I–X}^{\cdot} \xrightarrow{k_3} E \quad (37)$$

As in the first model the initial set of equations corresponding to the mechanism in Scheme 3 has been reduced to four equations by applying the steady-state aproximation for $A^{\cdot}$, $A(O_2)OO^{\cdot}$ and E-II:

$$d[E]/dt = k_3[E\text{-I–X}^{\cdot}] - k_1[E][AOOH] \quad (38)$$

$$d[E\text{-I}]/dt = k_1[E][AOOH] - k_{2a}[E\text{-I}] \quad (39)$$

$$d[E\text{-I–X}^{\cdot}]/dt = k_{2a}[E\text{-I}] - k_2[E\text{-I–X}^{\cdot}][AH] - k_3[E\text{-I–X}^{\cdot}] \quad (40)$$

$$d[AOOH]/dt = k_2[E\text{-I–X}^{\cdot}][AH] - k_1[E][AOOH] \quad (41)$$

Fig. 9 shows how the rate parameters k_1, k_{2a}, and k_2 affect the shape of the kinetic trace according to the mechanism in Scheme 3. It was assumed that k_3 is the same as in the first model (3×10^{-3} s^{-1}). In all theoretical curves shown, except one, k_1 has an assigned value of 8×10^7 M^{-1} s^{-1}, close to what was experimentally determined for 15-HPETE [14];

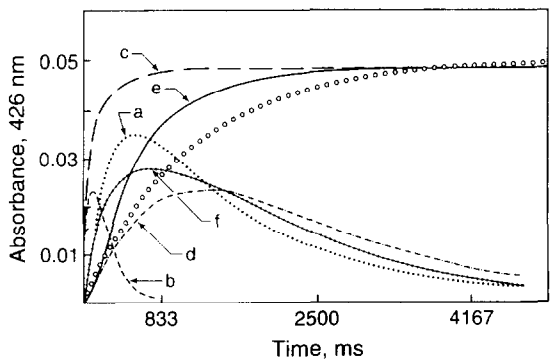

Fig. 9. Simulated time courses according to the mechanism in Scheme 3. (○) Exponential trace for experimental $k_{obs} = 0.89$ s^{-1}. (a–f): Theoretical curves for the same k_{obs} and initial conditions ($[AH]_0 = 5.5$ μM, $[A(O_2)OOH]_0 = 0.25$ μM, and $[E]_0 = 0.25$ μM). Combinations of the rate constants were as follows: (a) $k_1 = 8 \times 10^7$ M^{-1} s^{-1}, $k_2 = 1.2 \times 10^5$ M^{-1} s^{-1}, $k_{2a} = 6.5$ s^{-1} and $k_3 = 5 \times 10^{-1}$ s^{-1}; (b) k_1, k_2 and k_3 as in (a), $k_{2a} = 65$ s^{-1}; (c) k_1, k_{2a} and k_3 as in (b), $k_2 = 1 \times 10^2$ M^{-1} s^{-1}; (d) k_1, k_2 and k_3 as in (a), $k_{2a} = 1.2$ s^{-1}; (e) k_1 and k_3 as in (a), $k_{2a} = 2$ s^{-1} and $k_2 = 1.2 \times 10^3$ M^{-1} s^{-1}; (f) $k_1 = 1.4 \times 10^7$ M^{-1} s^{-1}, $k_2 = 1.2 \times 10^5$ M^{-1} s^{-1}, $k_{2a} = 65$ s^{-1} and $k_3 = 5 \times 10^{-3}$ s^{-1}.

as we showed, this is a good estimate in the first cyclooxygenase model. The values for k_{2a} and k_2 were combined differently; under no conditions could a good fit with the experimental trace be obtained. Furthermore, for the values of k_1 and k_{2a} as determined experimentally at 1° C [4] and for the k_2 and k_3 with the most realistic values, both the formation and disappearance of the intermediate II would be faster than what was actually observed at 30° C (Fig. 9, curve f).

4. Discussion

4.1. Initial conditions in the pre-steady-state kinetic measurements

Since the detection of the tyrosyl radical [3] there has been controversy about its role in catalysis [18–20]. It has been postulated that this enzyme species plays a key role in the initiation of the cyclooxygenase reaction by abstracting the 13-*pro*-S hydrogen atom from 20:4. However, the kinetic mechanism of the cyclooxygenase reaction had never been studied in detail. Probably the most important reason is the instability of the enzyme intermediates which had limited the use of transient-state techniques. The problem is complicated by the fact that the tyrosyl radical has an identical Soret spectrum with compound II and that similar spectral changes have been observed in the reactions of PGH synthase with both hydroperoxides and 20:4 [1,3,4].

Another part of the problem originates in the sensitivity of 20:4 to autooxidation so that small amounts of contaminant hydroperoxide are always present in its solutions. Often very rigid purification procedures [21] did not completely remove the contaminant hydroperoxide from 20:4; there was always some trace amount present capable of initiating the cyclooxygenase reaction. In our preliminary experiments we found that the use of purified 20:4 makes the pre-steady-state kinetic measurements very uncertain: the change in absorbance at 426 nm usually proceeded in more than a single step and this was accompanied with poor reproducibility. This happened because at low initial hydroperoxide concentration, an incomplete formation of compound I occurred followed by its conversion to more than one

species, i.e., to compound II and compound I–tyrosyl radical. With unpurified 20:4 samples single exponential traces were obtained (Fig. 2) with a satisfactory reproducibility which indicated that hydroperoxide concentration was constant and in excess of the enzyme so that the pseudo-first-order conditions were satisfied for all three substrates, hydroperoxide, oxygen, and 20:4. For the series of the pre-steady-state experiments with 20:4, the amount of oxygen was always constant (230 μM at 30° C) but the amount of contaminant hydroperoxide changed every time the amount of 20:4 was changed. In this situation the pre-steady-state kinetics is affected by both hydroperoxide and 20:4.

The initial conditions in our pre-steady-state experiments with 20:2 were adjusted in such a way that the effects of the fatty acid were fully separated from the effects of the hydroperoxide. We proceeded in the opposite direction from what has been a common procedure: instead of purifying fatty acid from the traces of hydroperoxide we oxidized a series of 20:2 solutions for different periods of time so that we were able to vary the ratio of hydroperoxide and 20:2 in stock solutions and keep the hydroperoxide concentration constant. For this approach, 20:2 was chosen as an alternative to 20:4. Although it utilizes one molecule of oxygen (the oxygenase reaction) it is a reasonable good substrate for the enzyme and identical changes in the enzyme spectra were obtained to those with 20:4 (Fig. 1), indicating that they probably share the same reaction mechanism. Furthermore, its hydroperoxide is a conjugated diene species that can be conveniently measured spectrophotometrically at 235 nm [6,7]. There is no more convenient method to measure the initial residues of the hydroperoxide in fatty acid solutions. In the past a polarographic procedure was used to measure the lipid peroxide concentrations by following the length of the lag phases in a cyanide-treated PGH synthase–cyclooxygenase reaction [22] but the latter method is less convenient than the spectrophotometric method.

4.2. The inhibition of the compound I reaction with 20:4 by indomethacin and 22:6

The effects of the cyclooxygenase inhibitors on the increase in absorbance at 426 nm (Fig. 2) can be explained as follows: indomethacin and 22:6 prevent the reaction of compound I with 20:4 by competing with 20:4 for the same binding site. The two inhibitors have similar dissociation constants for the initial binding to the enzyme but the overall mechanisms of the inhibition are different [16]. For 22:6, the inhibition is rapid and reversible while for indomethacin a rapid, reversible binding is followed by an irreversible first-order decay of an enzyme–inhibitor complex [16]. This explains why the inhibition of the compound I reaction with 20:4 was more effective with indometacin than with 22:6.

It has been demonstrated by e.p.r. studies [15,23] that indomethacin and other cyclooxygenase inhibitors did not prevent the formation of tyrosyl radical signals although they inhibited the cyclooxygenase reaction. There are two distinct tyrosyl radical species detected during reactions with hydroperoxides or 20:4, a transient doublet which is replaced by a narrow singlet at longer times [3,15,24]. A third tyrosyl radical signal has also been detected as a broad singlet in the presence of indomethacin or under conditions that enhance self-inactivation [15,24]. Its identity has been recently solved [25]. The broad singlet is not a distinct tyrosyl radical species but a composite of the narrow singlet and the doublet originating from the same tyrosyl residue [25]. The kinetics of the formation of doublet and singlet radical species did not correlate to the time course of 20:4 oxidation [24] or only the doublet is formed at a rate high enough to have catalytic competence in the cyclooxygenase reaction [15,23]. Since the doublet radical is transforming to the singlet radical and since both probably originate from the same, not from two different tyrosyl residues [25], these results are more in agreement with a role for the tyrosyl radical in oxidative auto-inactivation, not in catalysis. Our results are consistent with these findings. One might anticipate that if the tyrosyl radical were the species formed from compound I then indomethacin would have no effect on k_{obs}, which is not the case (Fig. 2). Both indomethacin and 22:6 prevented the conversion of compound I to intermediate II. Thus, intermediate II probably is not the compound I–tyrosyl radical. Rather it is either compound II or some unidentified compound I–protein radical having identical spectroscopic properties to those of compound II. In addition, Mn(III)–PGH

synthase does not generate tyrosyl radicals but some unidentified protein radical and still is a very active cyclooxygenase [24,26]. The authors of the tyrosyl radical hypothesis agree that some unidentified amino acid radical instead can play an active role in PGH synthase catalysis [18]. Recently it was shown that mutation of tyrosine 385 with phenyl alanine (Y385F) abolished the cyclooxygenase activity but did not prevent the formation of narrower singlet radical [27]. The isotopic replacement with predeuterated tyrosine and phenyl alanine in the Y385F mutant established that the singlet radical originates from an unknown tyrosine residue. This questioned the number and the identity of tyrosyl residues participating in catalysis and/or inactivation. Nonetheless, the entity presented in our model as E-I–X$^{\cdot}$ (Schemes 1 and 2) can be either a tyrosyl radical or any other protein radical which has the compound II-like heme structure.

4.3. Mechanism of the PGH synthase cyclooxygenase and oxygenase reactions

Our pre-steady-state results and computer modelling revealed a unique mechanism for the oxidation of fatty acids (20:2 and 20:4) catalyzed by PGH synthase which lead to the formation of transient hydroperoxides (11-OOH–20:2 and PGG_2). According to our mechanism (Schemes 1 and 2) the heme group at the enzyme active site participates directly in all steps of the oxygenation reaction. The reaction of hydroperoxide with native enzyme leads to formation of the corresponding alcohol and compound I (the peroxidase reaction); compound I abstracts a hydrogen atom from the fatty acid producing compound II and fatty acid carbon radical (the initiation of the cyclo- and oxygenase reactions); the fatty acid carbon radical converts to the corresponding fatty acid hydroperoxyl radical after fast addition of one or two molecules of oxygen (the oxygenase and cyclooxygenase reactions). Compound II is a transient species under aerobic conditions which undergoes fast hydrogen atom abstraction at one protein residue by the hydroperoxyl radical and compound I–protein radical and corresponding hydroperoxide are formed (the completion of the cyclo- and oxygenase reactions). Overall, the conversion of the enzyme species is from E → E-I → E-II → E-I–X$^{\cdot}$. The change in concentration of E, E-I, and E-I–X$^{\cdot}$ species as a function of time is shown in Fig. 6B. By using two different types of fatty acids we showed that the conversion of E-I is a function of fatty acid concentration, a relationship typical for bimolecular reactions. We showed that E-II is also formed as a transient species under aerobic conditions. Since E-II has an identical spectra to that of E-I–X$^{\cdot}$ no further distinctions between them were possible. We showed that the kinetic mechanism which includes the spontaneous E-I → E-I–X$^{\cdot}$ reaction does not fit the experimentally observed kinetics (Fig. 9).

The magnitudes of the rate constants for the reactions of lipid peroxides with native enzyme, k_1, are known from earlier transient state and steady-state studies [4,12,14,17]. Here for the first time we report the value for the k_1 obtained from a combination of the pre-steady-state experiments and computer modelling. We showed that the rate constant k_1 is 4 x10^7 M^{-1} s^{-1} for the reaction of the native enzyme with HOO–20:2 and 8 x10^7 M^{-1} s^{-1} for the reaction with HOO–20:4. The value of $k_1 = 7.1 \times 10^7$ M^{-1} s^{-1} obtained under steady-state conditions with 15-HPETE, also a hydroperoxide product of 20:4 [14], is the closest value to those predicted from our pre-steady-state modelling. Thus, for the first catalytic step (the peroxidase reaction of the native enzyme) our pre-steady-state model agrees with the previous studies. However, the pre-steady-state kinetics disagrees with the previous hypothesis for the following catalytic step, i.e., the initiation of the cyclooxygenase reaction.

According to our model (Schemes 1 and 2), the reaction of compound I with fatty acid (E-II formation) appeared to be two orders of magnitude slower than the reaction of lipid peroxide with native enzyme (E-I formation). Our model predicts that the oxygen-related steps which occur after the reaction of compound I with fatty acid do not have an effect on the observed rate. The rate of E-I–X$^{\cdot}$ return to the native enzyme E is a secondary reaction not significant on the time scales of our experiments. For the computer simulations we used an arbitrary low value of $k_3 = 3$ x10^{-3} s^{-1}. Thus, by modelling the cyclo- and oxygenase reactions we find out that we can apply more simple kinetic relationships for the 20:4 and 20:2 reactions with E-I. Initially we only

knew that for the reaction with 20:2 the pseudo-first-order conditions were satisfied. Without modelling we would not be able to find out that the same is true for the reaction with 20:4 and to see that oxygen concentration and the rate constants for the oxygen related steps do not affect the rate of the reaction of E-I with fatty acid. Finally, by modelling we showed the most probable sequence of events (Schemes 1 and 2) which does not agree with the tyrosyl radical hypothesis (Scheme 3).

Under pseudo-first-order conditions, the observed reaction rate is the rate of the rate controlling step and the modelling showed that this is the reaction of compound I with fatty acid:

$$-\mathrm{d[E\text{-}I]}/\mathrm{d}t = k_2[\mathrm{AH}][\mathrm{E\text{-}I}]$$

$$k_{\mathrm{obs}} = k_2[\mathrm{AH}]$$

Hence, the slopes of the curves in Figs. 4 and 7 represent the apparent second-order rate constant, k_2, for the reaction of 20:2 and 20:4 with PGH synthase compound I. Within experimental error, the k_2 values from the experiments (1.2×10^5 M^{-1} s^{-1} for 20:4 and 2.5×10^5 M^{-1} s^{-1} for 20:2) and those obtained by the computer simulations are identical.

The spontaneous decay of compound I is insignificant in both 20:2 and 20:4 experiments since no significant intercepts were observed in the plots of k_{obs} versus [fatty acid] (Figs. 4 and 7). At least when the hydroperoxide concentration was constant and 10-fold in excess of the enzyme concentration, as in the experiments with 20: 2 (Fig. 4), the intercept would be very obvious if the intramolecular electron transfer occurred to transform compound I to the compound I–tyrosyl radical. One can conclude that the spontaneous tyrosyl radical formation predicted from the kinetics of the reactions of native enzyme with hydroperoxides only [4] is not significant and does not occur simultaneously with the reaction of compound I with fatty acid. This could indicate that the fatty acid prevents the spontaneous decay of compound I to the tyrosyl radical [3,4].

A limit of our model is that it predicts a shorter lag phase than is observed experimentally (Figs. 6 and 8). We assumed that compound II is in a steady state throughout the course of the reaction, whereas in the lag phase compound II has not yet attained its steady-state value.

5. Conclusions

Our pre-steady-state experiments and kinetic modelling reveal the identity of the oxidizing agent for the initiation of fatty acid oxygenation to be compound I, not the compound I–tyrosyl radical. Rather the protein radical species does form simultaneously with hydroperoxide as a result of compound II reaction with the hydroperoxyl radical. We do not rule out the possibility that the protein radical can have a role in the events after the formation of the first molecule of hydroperoxide.

We provide kinetic evidence for a direct involvement of the heme prosthetic group in all steps of the oxygenation reaction (hydroperoxide formation). This indicates that the binding site of the fatty acid might be in a close proximity to the heme to allow the direct electron transfer from fatty acid to compound I intermediate, not remote from the heme as suggested in a model of the PGH synthase active site [28]. This interpretation is consistent with the recent X-ray crystal structure of PGH synthase [29]. Tyr^{385} is positioned near the edge of the heme and in the upper portion of the hydrophobic fatty acid binding site. Because of the low resolution of the enzyme–inhibitor complex the interaction of 20:4 with the active centre is not clear but a stereochemically built model indicates that C-13 of 20:4 would be bound in the vicinity of Tyr^{385} and consequently in the vicinity of the heme. From our kinetic study it is very likely that the fatty acid donates an electron directly to the porphyrin cation radical and a proton to a near basic amino acid residue of compound I.

Further structural models of 20:4 binding are needed for PGG_2 binding in the fatty acid channel. This will be useful in the elucidation of the position and the orientation of the Tyr^{385} and other protein residues relative to the heme and the $\mathrm{PGG}_2^{\cdot}$ radical. The most prominent catalytic role of the enzyme is to stabilize the transient free radical intermediates and their transition states. The hydroperoxyl radicals are probably situated in the fatty acid channel before the first hydroperoxide molecule is formed. We postulate that the tyrosyl radical is formed simultaneously with the first molecule of hydroperoxide. Thus all cyclooxygenase steps occur in the hydrophobic channel. The neutral hydroperoxide molecule is relo-

cated to the peroxidase binding site after formation of the compound I–protein radical.

The kinetic mechanism proposed in this study will require further verification, particularly under anerobic conditions where the reaction of E-I + AH → E-II can be isolated from the oxygen-related steps. It will be also important to see whether the classical electron donors promote or inhibit the compound I reaction with fatty acids or have no effect.

The question of the rate controlling step in the overall cyclooxygenase reaction still remains open. The second-order rate constant of the overall conversion of 20:4 to PGG_2 has been estimated to be 4×10^4 M^{-1} s^{-1} [30] which is more than one order of magnitude lower than k_2. This suggests that step(s) after formation of the intermediate E-I–X$^{\cdot}$, are the most plausible candidates for the rate controlling step in the overall reaction. It has been shown before [12], and in our preliminary experiments, that the return of the intermediate II to the native enzyme coincides with the rate of the oxygen consumption in the PGH synthase–cyclooxygenase reaction.

Similar results were obtained with Mn(III)–PGH synthase [7]. It was suggested that formation of the Mn(IV) oxidized state which relates to Fe(IV) oxidized state in E-I–X$^{\cdot}$ and/or to E-II, preceded or coincided to the hydroperoxide HOO–20:2 formation. This indicates that Fe(IV) species, E-I–X$^{\cdot}$ and/or E-II, can be competent intermediates for the rate controlling step in the overall oxygenation. A Mn(V) species, which corresponds to the Fe(V) state of E-I, was not detected. E-I–X$^{\cdot}$ could be a separate and distinct oxidizing agent from E-I and E-II but its role is still uncertain. In this study we showed that the compound I reaction with 20:4 and 20:2 is not complicated by the enzyme inactivation in a broad range (one order of magnitude) of 20:4 and 20:2 concentrations. However, the disappearance of intermediate II after the steady-state has been reached is accompanied by an extensive enzyme bleaching (Fig. 2). Even though the reaction of intermediate II with fatty acids is slower and more convenient for kinetic measurements than the compound I reaction with fatty acids, the interpretation of the kinetic results is more challenging. Intermediate II appears to be start of the pathway of auto-inactivation. This pathway has not yet been studied in detail but is important for an understanding of the overall oxygenation mechanism.

References

[1] A.-M. Lambeir, C.M. Markey, H.B. Dunford and L.J. Marnett, J. Biol. Chem., 260 (1985) 14894.

[2] H.B. Dunford, in J. Everse, K. Everse and M.B. Grisham (Editors), Peroxidases in Chemistry and Biology, Vol. 2, CRC Press, Boca Raton, FL, 1991, p. 1.

[3] R. Karthein, W. Nastainczyk and H.H. Ruf, Eur. J. Biochem., 166 (1987) 173.

[4] R. Dietz, W. Nastainczyk and H.H. Ruf, Eur. J. Biochem., 171 (1988) 321.

[5] M. Bakovic and H.B. Dunford, Biochemistry, 33 (1994) 6475.

[6] G. Graff, L.A. Anderson and L.W. Jaques, Anal. Biochem., 188 (1990) 38.

[7] R. Odenwaller, K.R. Maddipati and L.J. Marnett, J. Biol. Chem., 267 (1992) 13863.

[8] L.J. Marnett, P.H. Siedlik, R.C. Ochs, W.R. Pagels, M. Das, K.V. Honn, R.H. Warnock, B.E. Tainer and T.E. Eling, Mol. Pharmacol., 26 (1984) 328.

[9] I.D. MacDonald and H.B. Dunford, J. Inorg. Biochem., 37 (1989) 35.

[10] R.J. Kulmacz and W.E.M. Lands, J. Biol. Chem., 259 (1984) 6358.

[11] J. Robinson and J.M. Cooper, Anal. Biochem., 33 (1970) 390.

[12] I.D. MacDonald and H.B. Dunford, Biochem. Cell Biol., 67 (1989) 301.

[13] Y. Hsuanyu and H.B. Dunford, Arch. Biochem. Biophys., 281 (1990) 282.

[14] R.J. Kulmacz, Arch. Biochem. Biophys., 249 (1986) 273.

[15] R.J. Kulmacz, Y. Ren, A.-L. Tsai, G. Palmer, Biochemistry, 29 (1990) 8760.

[16] R.J. Kulmacz and W.E.M. Lands, J. Biol. Chem., 260 (1985) 12572.

[17] P.J. Marshall and R.J. Kulmacz, Arch. Biochem. Biophys., 266 (1988) 162.

[18] H.H. Ruf, U. Raab-Brill and C. Blau, Biochem. Soc. Trans., 21 (1993) 739.

[19] W.L. Smith, T.E. Eling, R.J. Kulmacz, L.J. Marnett and A. Tsai, Biochemistry, 31 (1992) 3.

[20] W.L. Smith and L.J. Marnett, Biochem. Biophys. Acta, 1083 (1991) 1.

[21] Y. Hsuanyu and H.B. Dunford, Anal. Biochem., 198 (1991) 174.

[22] P.J. Marshall, M.A. Warso and W.E.M. Lands, Anal. Biochem., 145 (1985) 192.

[23] R.J. Kulmacz, G. Palmer and A.-L. Tsai, Mol. Pharmacol., 40 (1991) 833.

[24] G. Lassman, R. Odenwaller, J.F. Curtis, J.A. DeGray, R.P. Mason, L.J. Marnett and T.E. Eling, J. Biol. Chem., 266 (1991) 20045.

[25] J.A. DeGray, G. Lassman, J.F. Curtis, T.A. Kennedy, L.J. Marnett, T.E. Eling and R.P. Mason, J. Biol. Chem., 267 (1992) 23583.
[26] R.J. Kulmacz, G. Palmer, C. Wei and A.-L. Tsai, Biochemistry, 33 (1994) 5428.
[27] A.-L. Tsai, L.C. Hsi, R.J. Kulmacz, G. Palmer and W.L. Smith, J. Biol. Chem., 269 (1994) 5085.
[28] T. Shimokava and W.L. Smith, J. Biol. Chem., 260 (1991) 6168.
[29] D. Picot, P.J. Loll and M. Garavito, Nature (London), 367 (1994) 243.
[30] Y. Hsuanyu and H.B. Dunford, J. Biol. Chem., 267 (1992) 17649.